Precambrian Research 225 (2013) 77–85

Contents lists available at SciVerse ScienceDirect

Precambrian Research

journal homepage: www.elsevier.com/locate/precamres

Greigite from carbonate concretions of the Ediacaran Doushantuo Formation in South China and its environmental implications

Jin Dong[a,b], Shihong Zhang[a,*], Ganqing Jiang[c], Haiyan Li[a], Rui Gao[b]

[a] State Key Laboratory of Geological Process and Mineral Resources, China University of Geosciences, Beijing 100083, PR China
[b] Institute of Geology, Chinese Academy of Geological Sciences, Beijing 100037, PR China
[c] Department of Geoscience, University of Nevada, Las Vegas, NV 89154-4010, USA

ARTICLE INFO

Article history:
Received 23 June 2011
Received in revised form 19 March 2012
Accepted 21 March 2012
Available online 3 April 2012

Keywords:
Greigite
Carbonate concretion
Doushantuo Formation
Ediacaran
South China
Early diagenesis

ABSTRACT

Greigite (Fe_3S_4) is a ferrimagnetic iron sulfide that commonly forms as a precursor of pyrite in anoxic environments where the supply of reactive Fe outpaces that of sulfide (H_2S and HS^-). Because of its metastability and sensitivity to redox changes during burial, greigite has been rarely documented in rocks older than the Cretaceous. Here we report well-preserved greigite in carbonate concretions of the upper Doushantuo Formation (ca. 551 Ma) in the Yangtze Gorge area, South China. Greigite in the carbonate concretions coexists with anhedral and framboidal pyrite, and is distributed in clay-rich carbonates with card-house microtextures and dolomitic spherical structures indicative of early diagenetic formation during shallow burial. Preservation of greigite in carbonate concretions of the upper Doushantuo Formation implies that these concretions maintained a closed micro-system since their formation and that they provide information about the ancient depositional and early diagenetic environments.

1. Introduction

Greigite is a ferrimagnetic iron sulfide mineral that has a similar spinel crystal structure to magnetite (Skinner et al., 1964). It usually forms as a metastable precursor of pyrite in anoxic sedimentary environments where dissolved iron provided by reduction of reactive iron oxides outpaces sulfide supply (Karlin and Levi, 1983; Berner, 1984; Canfield and Berner, 1987; Karlin, 1990a,b; Kao et al., 2004). Because of its ferrimagnetic attributes, greigite has been widely documented in paleomagnetic and paleoenvironmental studies (e.g. Snowball and Thompson, 1988; Snowball, 1991; Roberts and Turner, 1993; Florindo and Sagnotti, 1995; Horng et al., 1998; Jiang et al., 2001; Roberts et al., 2005; Rowan and Roberts, 2005, 2006, 2008; Sagnotti et al., 2005). In Cenozoic successions, greigite has been found in a wide range of depositional environments, such as estuaries and deep-sea fans (Kasten et al., 1998), hemipelagic deposits on continental shelves and deep-water basins (Berner, 1984; Horng et al., 1992; Lee and Jin, 1995; Sagnotti and Winkler, 1999; Oda and Torri, 2004), and gas hydrate systems (Housen and Musgrave, 1996; Larrasoaña et al., 2007). However, because greigite can be poorly crystalline and sensitive to redox changes and to elevated temperatures during deeper burial, its preservation and identification in old sedimentary successions is often difficult.

It has been inferred that greigite was part of an iron monosulfide membrane that served as a catalyst between fluids in a Hadean submarine hydrothermal redox front that may have enabled emergence of life on Earth (Russell et al., 1994; Russell and Hall, 1997), but either such early greigite has not been preserved in the geological record or it has not been discovered. The oldest strata reported to host hydrothermal greigite within siderite nodules are of Permo-Carboniferous age (Krupp, 1991, 1994). In this case, the preservation of greigite suggested that siderite nodules could provide protection from later oxidation (Krupp, 1994). Greigite has also been reported from Cretaceous strata of northern Alaska (Reynolds et al., 1994) and Peru (Linder and Gilder, 2011), but some of those reported greigites might have formed during late diagenesis, much younger than Cretaceous.

In this paper, we report the occurrence of greigite in carbonate concretions of the Ediacaran Doushantuo Formation in South China. These carbonate concretions are hosted in the black shales of the uppermost Doushantuo Formation that has been dated at ca. 551 Ma (Condon et al., 2005; Zhang et al., 2005). If the greigite in these concretions were formed close to the time of deposition, this would be the oldest documented occurrence of greigite in the geological record. We test this possibility and the potential paleoenvironmental information that can be provided by the occurrence of greigite.

* Corresponding author at: China University of Geosciences, Beijing, 29 Xueyuan Road, Haidian, Beijing 100083, PR China. Tel.: +86 10 82322257; fax: +86 10 82321983.
E-mail address: shzhang@cugb.edu.cn (S. Zhang).

0301-9268/$ – see front matter © 2012 Elsevier B.V. All rights reserved.
http://dx.doi.org/10.1016/j.precamres.2012.03.010

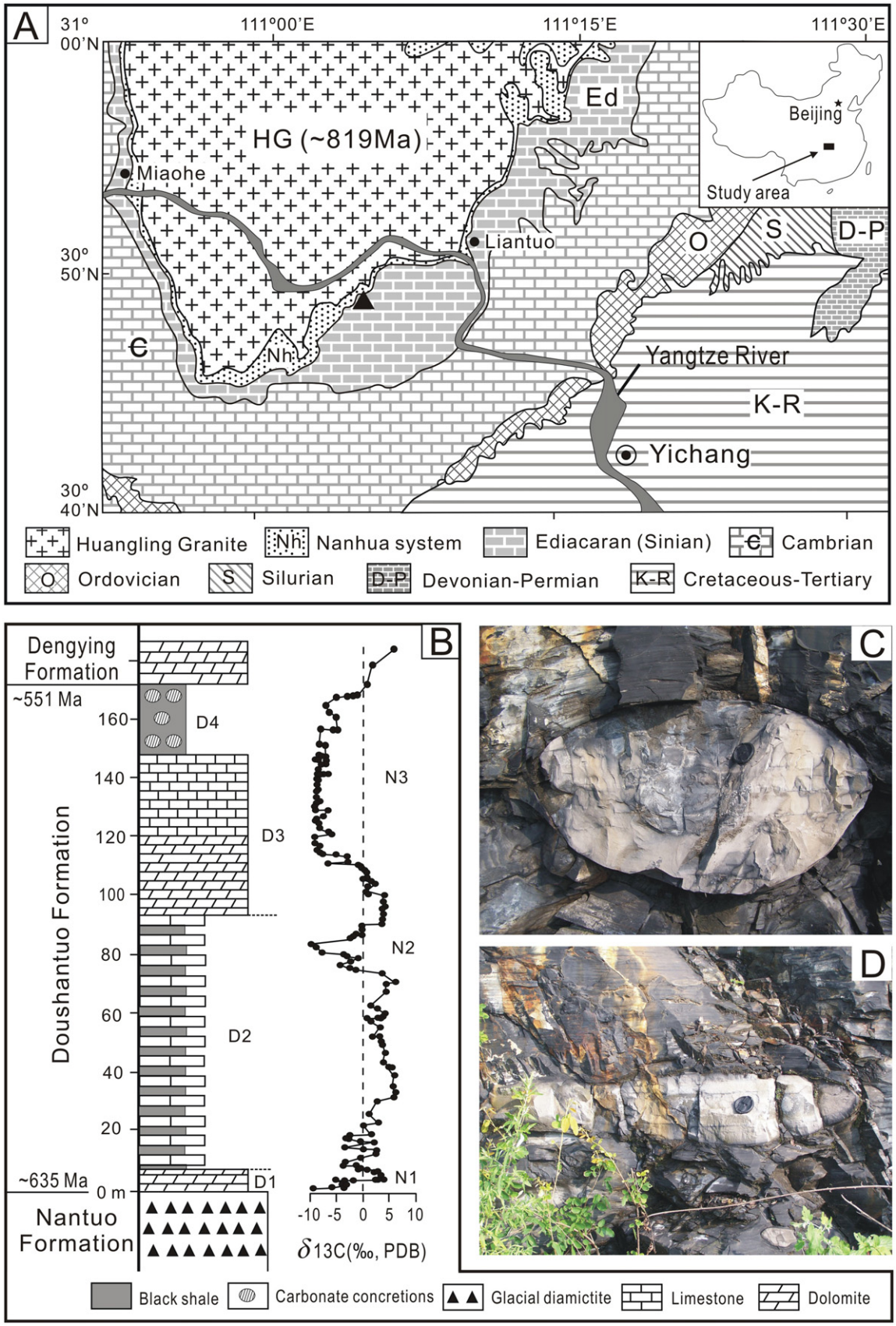

Fig. 1. (A) Simplified geological map of the Yangtze Gorge area (after Zhang et al., 2005) with location of the studied section (closed triangle). (B) Stratigraphic column of the Doushantuo Formation (after Jiang et al., 2007). (C and D) Field photographs of concretions (Camera lens cap in C and D is 65 mm across).

2. Geological background

The study sections are located in the Yangtze Gorge area of Hubei province (Fig. 1A). The Neoproterozoic strata in this area unconformably overlie the ca. 820 Ma Huangling Granite and are composed of three parts: pre-Cryogenian (>725 Ma; Zhang et al., 2008a) siliciclastic rocks (Liantuo Formation), Cryogenian glaciogenic Nantuo Formation (~654–635 Ma, Zhang et al., 2008b, 2008c), and Ediacaran carbonate and shale (Doushantuo and Dengying formations). The Liantuo and Nantuo formations and their equivalent strata in South China are well dated and are thought to have been deposited in fluvial to shallow-marine environments of a southeast-facing rift margin, while the Ediacaran strata may represent deposits of a passive continental margin (Jiang et al., 2003a; Wang and Li, 2003).

Lithologically, the Doushantuo Formation in this area can be divided into four members (Zhu et al., 2003, 2007; Jiang et al., 2011) (Fig. 1B). The lowest member is the 3- to 6-m-thick "Doushantuo cap carbonate" (Jiang et al., 2003b, 2006a,b) that marks the base of the Ediacaran Period (Knoll et al., 2004) in South China and has been dated at 635.2 ± 0.6 Ma (Condon et al., 2005; Zhang et al., 2005). The second member consists of an up to 70-m-thick, interbedded black shale and shaley limestone with abundant pea-sized phosphorite-chert nodules. The third member is composed of ~70-m-thick, gray to dark dolomite and dolomitic limestone. In these two members, macroscopic animal embryo fossils, large acanthomorph acritarchs, and multicellular algae have been found (Zhang et al., 1998; Xiao, 2004; Yin et al., 2007; Zhou et al., 2007; McFadden et al., 2008, 2009; Liu et al., 2009). The fourth member consists of a 10-m-thick black shale that contains abundant carbonate concretions, which is the focus of this study. Macroscopic algae and putative animal fossils named as the Miaohe biota were found in this member (Ding et al., 1996; Zhang et al., 1998; Xiao et al., 2002). A volcanic ash bed near the top of this member yielded a U–Pb zircon age of 551 ± 0.7 Ma (Condon et al., 2005; Zhang et al., 2005).

Carbonate concretions in this fourth member of the Doushantuo Formation are usually isolated (Fig. 1C), but in some cases they align along the bedding plane (Fig. 1D). The hosting shale contains

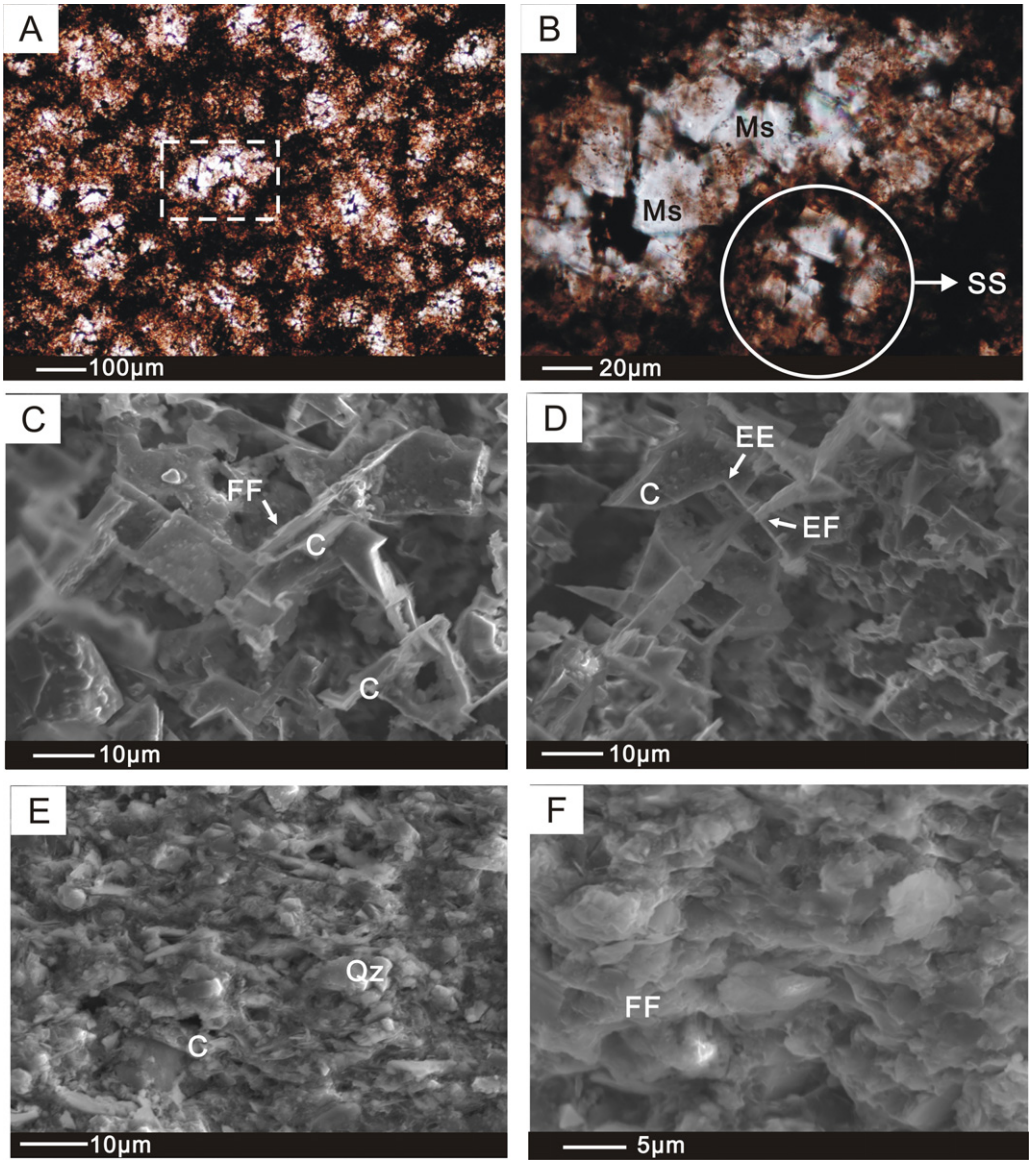

Fig. 2. Optical microscope and SEM images of concretions and host rocks. (A and B) Optical microscope images of concretions. (C and D) SEM images of concretion lightly etched with dilute hydrochloric acid, with house of card fabrics. (E and F) SEM images of host rocks with preferred alignment of clays. (B) is a magnified image from the dashed frame in (A). Ms, dolomite spar; C, clay; Qz, quartz; FF, face-to-face contact (of clay); EF, edge-to-face contact; EE, edge-to-edge contact; SS: spherical texture.

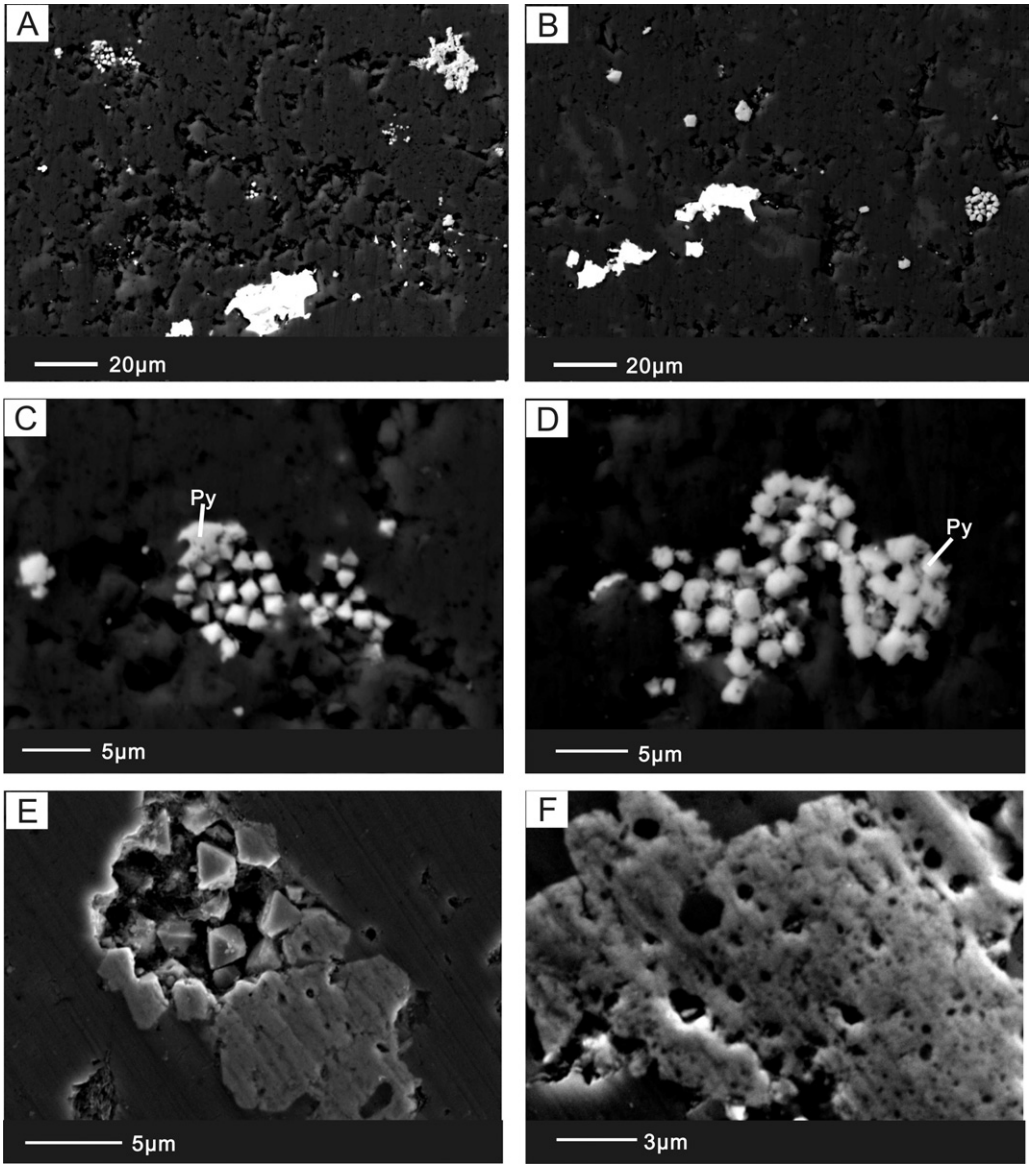

Fig. 3. Representative back-scattered electron images of pyrite in the concretions. (A and B) Anhedral and aggregated. (C and D) Pyrite aggregate, with cubic and octahedral crystals. (E and F) Anhedral pyrite, with many voids on its surface. Bright areas are pyrite or greigite and dark areas are background minerals, such as dolomite and quartz.

a clear foliation, while the concretions are usually massive with faint parallel laminations. Most of the carbonate concretions are spherical, with a small portion being ellipsoidal (Fig. 1C), oblate (Fig. 1D) or irregular. The size of these concretions varies generally from 0.1 to 0.5 m in diameter, with occasionally smaller or larger sizes. The boundaries between the host rock and concretions are distinct. Near the top of the Doushantuo Formation, a few horizons contain large layer-parallel concretions, some of which have clear sedimentary laminations. The host-rock bedding bends around the concretions, which indicates that the concretions formed before deep compaction (Fig. 1C).

3. Methods

Samples were collected from both concretions and host shales. Their mineral composition and microtextures were investigated using Scanning Electron Microscope (SEM), X-ray diffraction (XRD) and optical microscope observations. The SEM analyses were carried out at two laboratories: (1) A Hitachi S-3400N SEM, operated at 20 keV, equipped with a Link Analytical Oxford IE 350 for X-ray energy-dispersive spectrometer (EDS) analysis at the State Key Laboratory of Geological Process and Mineral Resources, China University of Geosciences, Beijing (Lab CUGB) and, (2) A Zeiss Supra 55 VP SEM, operated at 20 keV, with an EDS of Thermo Fisher Scientific Noran System six, at State Key Laboratory for Advanced Metals and Materials, University of Science and Technology Beijing (Lab USTB). Samples were coated with a thin layer of carbon to prevent charging. Iron sulfide minerals were identified using SEM and EDS on the basis of their chemical composition, high electron backscatter and microtextures (e.g., Jiang et al., 2001; Sagnotti et al., 2005; Weaver et al., 2002; Roberts et al., 2005). XRD measurements were carried out at the Institute of Petroleum Exploration and Development, PetroChina, Beijing.

4. Results

4.1. Mineral analyses

Mineral analyses demonstrate that the minerals in the host rocks of concretions are mostly quartz (~36%) and clay (~41%), with

minor amounts of K-feldspar (~4.2%), calcite (~3.6%), dolomite (~6.5%), and pyrite (~3.6%). The concretions are dominated by dolomite (~91%), with minor quartz (~2.6%), clay (~2.8%), and K-feldspar (~0.2%). Although the absolute mineral concentrations in the concretions differ from those of the host shales, the similarities of the type and proportion of detrital minerals in concretions and shales suggest that the concretions formed by authigenic carbonate cementation of detrital materials during early diagenesis (Dong et al., 2008). It should be noted that neither greigite nor pyrite could be identified using XRD because the percentage of greigite and pyrite is below the detection limit of the XRD in both concretions and host shales. EDS analysis shows that the dolomite only contained Ca, Mg, C and O but no Fe, which indicates that the carbonate cement is not siderite.

4.2. Microscope observations

Under the optical microscope, the most distinctive feature of the carbonate concretions is their spherical texture, which covers 80% of the fields of view (Fig. 2A and B). The spherical textures are about 100–200 μm across and are uniformly distributed in the concretions. They display similar features in orthogonal thin sections. Dolomite microspars with clear rhombic shape grow toward the center of the spheres, commonly forming an isopachous layer along the edge of the spheres. This texture is inferred to have been produced by carbonate-filled gas bubbles, which formed during organic matter decomposition near the sediment–water interface (Dong et al., 2008). Preservation of these spherical textures also indicates that carbonate cementation occurred during shallow-burial before compaction. A cement-supported framework may

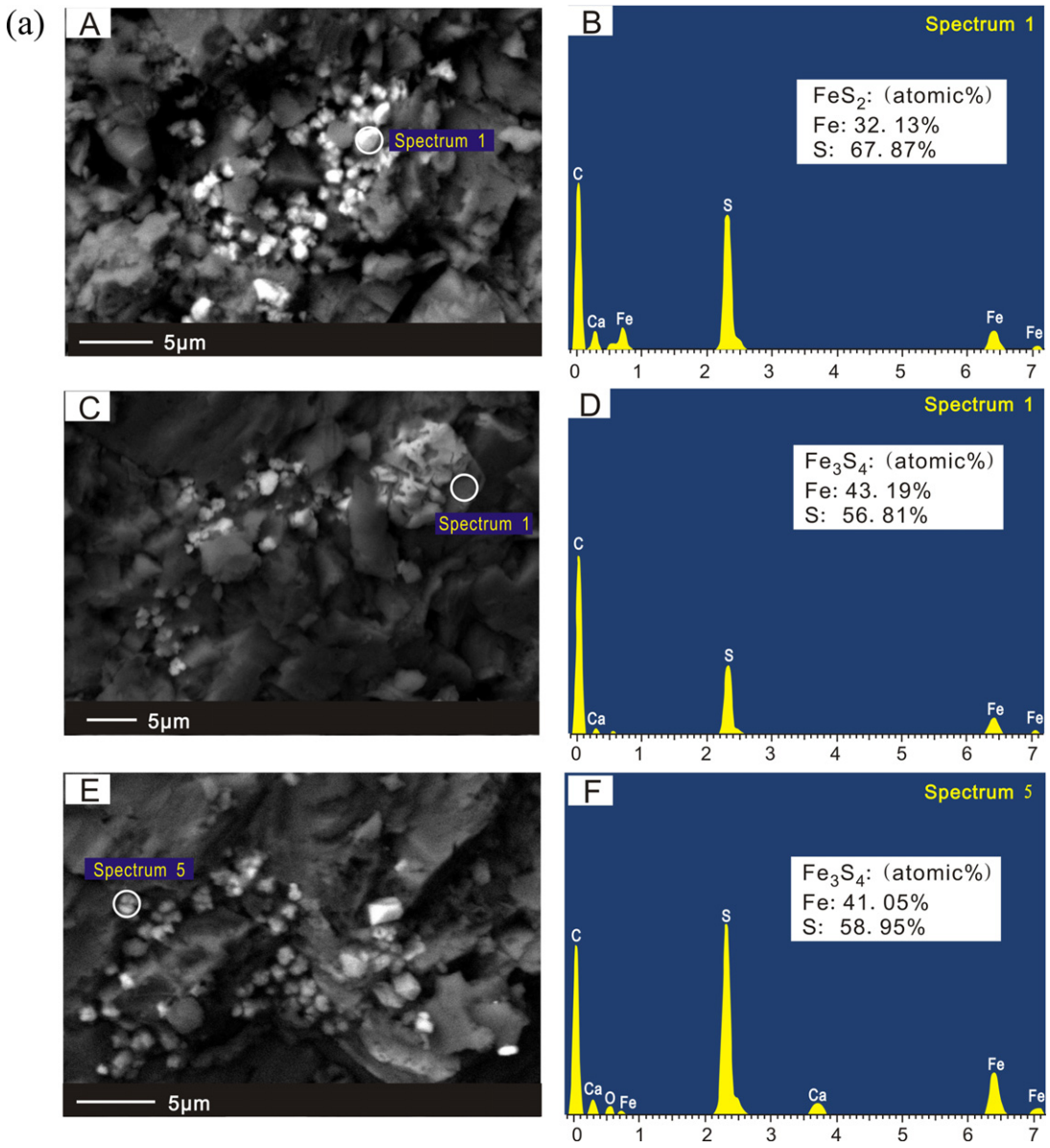

Fig. 4. (a) Representative back-scattered electron images (A, C and E) and EDS spectra (B, D and F) of pyrite and greigite in the studied carbonate concretions. White circle shows EDS analysis spot (all conducted at Lab CUGB, see text). (b) Representative back-scattered SEM images and EDS spectra of greigite in the concretions, A and B were analyzed at Lab CUGB; C, D, E and F were analyzed at Lab USTB.

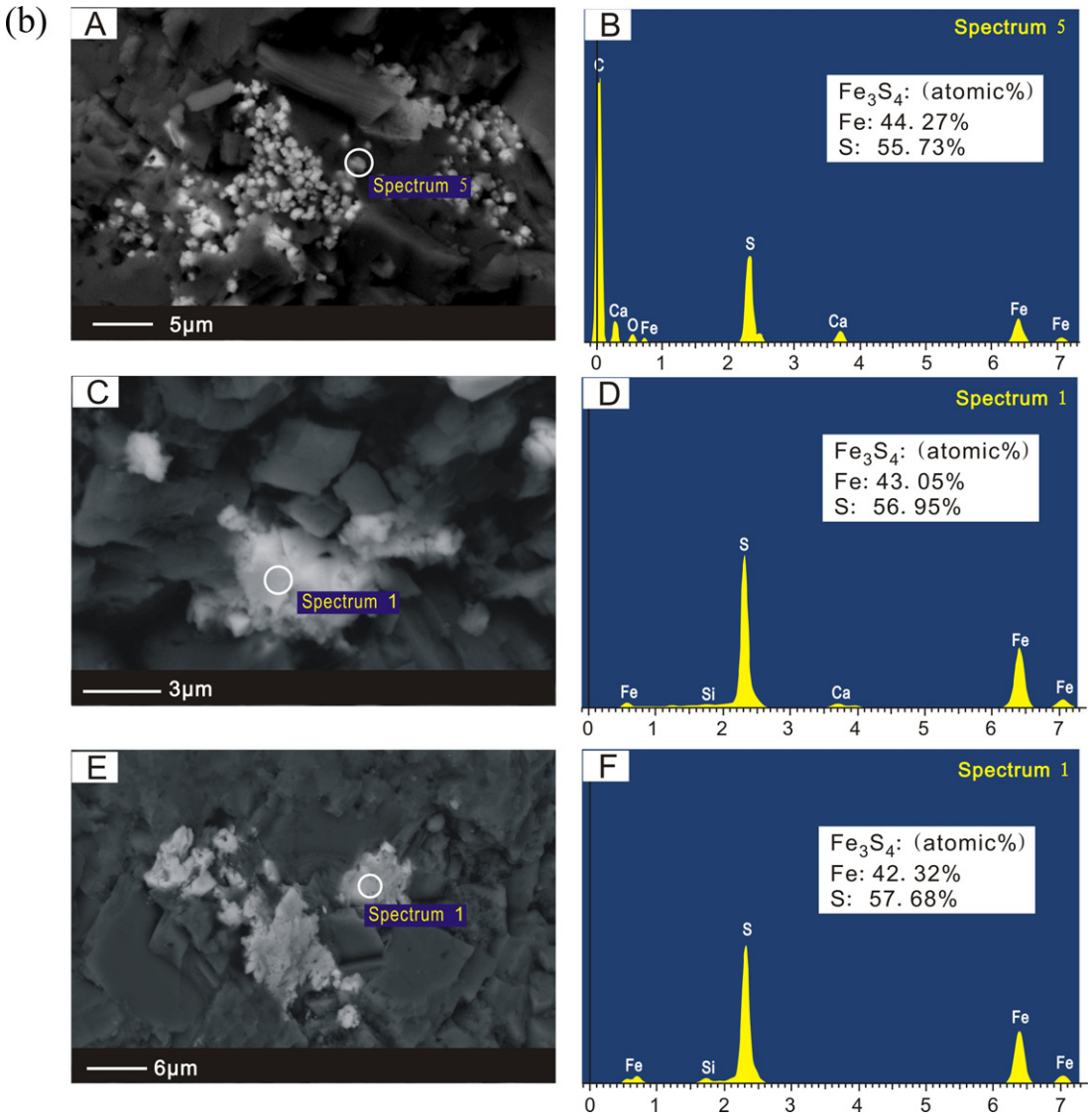

Fig. 4. (*Continued*)

have helped to maintain a closed system in carbonate concretions that prevented further chemical exchange between concretions and formation fluids (Raiswell, 1982; Raiswell and Fisher, 2000).

4.3. SEM observations

SEM observations indicate that the clay minerals are arranged randomly in the concretions with edge to face (EF), edge to edge (EE), and face to face (FF) modes of contact, which form a card-house fabric (Fig. 2C and D). This texture is common in modern clay-rich sediments (Zabawa, 1978; Woodland, 1984). The card-house clay fabric can be easily destroyed by compaction and exists only in the uppermost 0–3 m of sediments (Raiswell, 1976; Woodland, 1984). The well-preserved card-house fabric in the concretions indicates that these concretions formed before compaction and that carbonate cementation protected them from deformation during subsequent burial. This is consistent with field observations that the host-rock bedding bends around the concretions (Fig. 1C).

Several types of pyrite are observed under SEM in concretions and host rocks, including euhedral, anhedral and aggregate forms. Anhedral pyrite is the most common type in both concretions and host rocks (Fig. 3A and B), followed by pyrite aggregates, which are composed of crystals that are mostly cubic or octahedral in shape and about 0.1–1 μm in size (Fig. 3C and D). The pyrite aggregates are irregular in shape and do not display multiple growth generations. Anhedral pyrites are about 100–150 μm in size and have abundant, 0.1- to 1.5-μm-sized voids (Fig. 3E and F) on their surface, which are inferred to be relics left by organic matter decay or clay mineral decomposition (Fig. 3E and F). Pyrites are distributed in carbonate inter-crystal space or embedded in dolomite crystals. Their shapes are commonly influenced by the shape of dolomite. These features suggest that precipitation of pyrite was roughly synchronous with that of the dolomite.

Greigite is identified by crystal shape and distinctive chemical composition. Greigite (43% Fe:57% S) has a higher iron to sulfur ratio compared to pyrite (33% Fe:67% S), which makes it easy to identify using EDS analysis. Although monoclinic pyrrhotite (Fe_7S_8) (47% Fe:53% S) has a similar iron to sulfur ratio as greigite, these two phases usually have distinct morphologies. Pyrrhotite is typically platy, while greigite occurs as cubo-octahedral crystals (Roberts and Weaver, 2005). Greigite is dispersed in framboidal pyrite aggregates and anhedral pyrite (Fig. 4a and b). Compared to pyrite, greigite normally has brighter contrast due to its higher iron to sulfur ratio (Hoffmann, 1992). In some cases, however, greigite can also have slightly darker contrast because of its irregular scattering

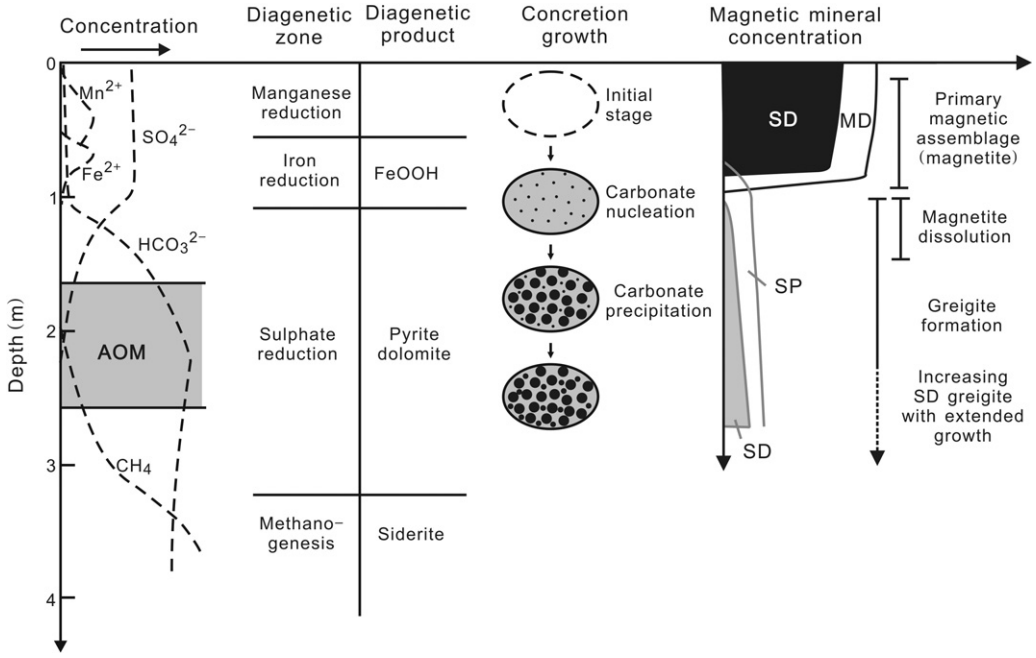

Fig. 5. Schematic geochemical classification scheme for modern marine sedimentary environments (adapted from Berner, 1981) and possible growth model for the Doushantuo concretions and greigite. SP, SD and MD indicate superparamagnetic, single-domain and multi-domain magnetic minerals (from Rowan et al., 2009).

surface and intergrowth of crystals (Jiang et al., 2001; Roberts and Weaver, 2005).

At Lab CUGB, the EDS of Hitachi S-3400N SEM may experience elemental interference from matrix or other minerals when analyzing small (<1 μm) greigites, so trace of other elements, such as Ca and O, could be captured in the EDS spectra (Fig. 4a and bB). In addition, some O might come from oxidation, too. In order to minimize such interferences, we observed fresh sample cuts and probed as many points as possible for statistical confirmation. Elemental analyses showed two distinctive, narrow iron peaks from iron sulfide minerals. One peak has iron content of 32–35%, which is consistent with pyrite; and the other has iron contents of 41–45%, consistent with greigite. The narrow iron peaks indicate that oxidation of iron sulfide is negligible, otherwise Fe/S ratios would be more scattered.

5. Discussion

Studies of modern organic-rich marine sediments indicate that, below the water–sediment interface, the sedimentary column can be divided into several diagenetic zones according to the reactants and products. Organic matter is oxidized through a progression of oxidants that produced a dissolved oxygen zone, a nitrate reduction zone, a manganese reduction zone, an iron reduction zone, a sulfate reduction zone and a methanogenesis zone (Fig. 5) (Berner, 1981; Roberts and Weaver, 2005).

According to conventional views of steady-state diagenesis, iron sulfide usually forms during early diagenesis at shallow burial depths, where detrital iron-bearing minerals react with hydrogen sulfide (H_2S) to produce pyrite (Karlin and Levi, 1983; Canfield and Berner, 1987; Karlin, 1990a,b). Greigite is an intermediate phase in this reaction (Berner, 1984; Wilkin and Barnes, 1997; Hunger and Benning, 2007) and its preservation is favored by high concentrations of reactive iron and low concentrations of organic carbon and H_2S (Kao et al., 2004). Rowan et al. (2009) demonstrated that greigite growth begins with nucleation of nanoparticles at the inferred position of the sulfate–methane transition and these nanoparticles progressively grow through the magnetic single-domain volume. This process is evident in several published records concerning the magnetic properties of greigite-bearing sediments (Karlin, 1990a; Tarduno, 1995; Yamazaki et al., 2003; Liu et al., 2004; Garming et al., 2005; Dillon and Bleil, 2006) and may be widespread in reducing sedimentary environments. Dissolved sulfide is normally completely consumed deeper in the sediment column (Berner, 1981; Kasten et al., 1998; Roberts and Weaver, 2005), so greigite should most commonly form in a brief period after deposition (e.g., Pye, 1981; Reynolds et al., 1999).

Greigite can also form during late diagenesis, which complicates studies of environmental magnetism and geomagnetic field behavior (e.g., Horng et al., 1998; Jiang et al., 2001; Roberts et al., 2005; Sagnotti et al., 2005; Rowan and Roberts, 2005, 2006, 2008). In the Doushantuo concretions, greigite and pyrite are distributed in dolomite inter-crystal space or embedded in dolomite crystals, which indicates that iron sulfides were precipitated roughly synchronously with dolomite formation. This raises question about the timing of greigite formation relative to the deposition of the Doushantuo Member IV shales. Dolomite, although abundant in the ancient rock record, is rarely found as primary carbonate precipitate in modern natural environments, which is known as the 'dolomite problem' (e.g., McKenzie, 1991). If the dolomite in the shale-hosted carbonate concretions was formed later in the diagenetic history, the pyrite and gregite closely associated with the dolomite may have also formed during late diagenesis. Laboratory experiments, however, have indicated that dolomite could form at low temperatures with sulfate-reducing bacterial involvement (Vasconcelos et al., 1995; Vasconcelos and McKenzie, 1997). Microbially mediated dolomite formation has been found in modern coastal lagoons (Vasconcelos and McKenzie, 1997) and in groundwater (Roberts et al., 2004). More recent finding of dolomite biomineralization in living coralline algae (Nash et al., 2011) also indicates that biologically initiated dolomite could be an important source of primary dolomite. Although the 'dolomite problem' in general is not fully solved, we believe that the dolomite (and greigite) in the Doushantuo concretions were formed during early diagenesis within the sulfate-reducing zone. This is consistent with the well-preserved card-house clay fabrics and spherical dolomite textures in the concretions, which indicate that the concretions were formed at very

shallow burial depth. The lack of iron in dolomite crystals suggests that dolomite and iron sulfides were formed in H_2S-rich microenvironment where iron was preferentially incorporated into sulfides rather than carbonate (e.g., the formation of siderite). Bicarbonate (HCO_3^-) required for dolomite precipitation could be produced in all diagenetic zones. In the nitrate, manganese and iron reduction zones, only minor amounts of HCO_3^- are produced so the concretion would have been in the nucleation stage only, while in the sulfate reduction zone, anaerobic organic carbon oxidation could generate significant amounts of HCO_3^-; this is generally considered as the major stage of carbonate concretionary growth (Raiswell, 1987, 1988; Lash and Blood, 2004; Hendry et al., 2006). At this stage, the generation of dissolved sulfide through sulfate reduction also promotes iron sulfide formation (Berner, 1984).

The preservation of greigite and card-house clay fabric in the concretions but not in the host shales suggests that the concretions served as a protecting armor for the minerals and textures during subsequent burial and diagenesis. Authigenic carbonate cementation created closed micro-systems so that formation fluids during burial were excluded from these concretions and further chemical reactions within the carbonate concretions were minimal (Raiswell, 1982; Raiswell and Fisher, 2000). In this consideration, the greigite from the Doushantuo concretions should have a potential for obtaining useful paleomagnetic information. However, caution should be taken not only because greigite has low unblock temperature (Roberts, 1995; Dekkers et al., 2000; Chang et al., 2008), but also because a reliable paleomagnetic pole requires robust field tests as well. Unfortunately, the Doushantuo Formation across the Yangtze platform has so far never passed a reversals test.

6. Conclusions

Using SEM and EDS analyses, greigite has been identified from carbonate concretions of the uppermost Doushantuo Formation (ca. 551 Ma). The association of greigite with well-preserved card-house clay fabric and spherical dolomite texture in these concretions indicates early diagenetic formation within the sulfate reduction zone. Authigenic carbonate cementation in these concretions created closed micro-systems that served as protecting armor for the minerals and textures during subsequent burial and diagenesis.

The presence of greigite in Precambrian concretions may have implications for paleoenvironmental and paleomagnetic studies. First, its occurrence confirms that greigite can persist for long geological periods, at least under special conditions such as within concretions. Second, the close association of greigite and clay microfabrics suggests formation during early diagenesis before compaction. The composition of pore fluids at that stage may have been close to that of seawater. Third, the presence of greigite may provide a reference for paleomagnetic studies. Primary greigite is usually formed within 2000 years after deposition (e.g. Pye, 1981; Canfield and Berner, 1987; Reynolds et al., 1999) and this time lag could be negligible compared to its subsequent geological history. If greigite in such environments can be demonstrated to have an early origin and carries a primary magnetization, paleomagnetic analysis of such rocks could be very useful.

Acknowledgments

Authors thank Andrew P. Roberts, Graham Shields, Maoyan Zhu and another reviewer for their constructive comments and suggestions. This work was jointly supported by 973 Program (2011CB808800), SinoProbe, NSFC projects 40921062, 40974035 and 40830316.

References

Berner, R.A., 1981. A new geochemical classification of sedimentary environments. Journal of Sedimentary Research 51, 359–365.
Berner, R.A., 1984. Sedimentary pyrite formation: an update. Geochimica et Cosmochimica Acta 48, 605–615.
Canfield, D.E., Berner, R.A., 1987. Dissolution and pyritization of magnetite in anoxic marine sediments. Geochimica et Cosmochimica Acta 51, 645–659.
Chang, L., Roberts, A.P., Tang, Y., Rainford, B.D., Muxworthy, A.R., Chen, Q.W., 2008. Fundamental magnetic parameters from pure synthetic greigite (Fe_3S_4). Journal of Geophysical Research 113, http://dx.doi.org/10.1029/2007JB005502.
Condon, D., Zhu, M., Bowring, S., Wang, W., Yang, A., Jin, Y., 2005. U–Pb ages from the Neoproterozoic Doushantuo Formation, China. Science 308, 95–98.
Dekkers, M.J., Passier, H.F., Schoonen, M.A.A., 2000. Magnetic properties of hydrothermally synthesized greigite (Fe_3S_4) – II. High- and low-temperature characteristics. Geophysical Journal International 141, 809–819.
Dillon, M., Bleil, U., 2006. Rock magnetic signatures in diagenetically altered sediments from the Niger deep-sea fan. Journal of Geophysical Research 111, http://dx.doi.org/10.1029/2004JB003540.
Ding, L., Li, Y., Hu, X., Xiao, Y., Su, C., Huang, J., 1996. Sinian Miaohe Biota. Geological Publishing House, Beijing (in Chinese).
Dong, J., Zhang, S.H., Jiang, G.Q., Zhao, Q.L., Li, H.Y., Shi, X.Y., Liu, J.L., 2008. Early diagenetic growth of carbonate concretions in the upper Doushantuo Formation in South China and their significance for the assessment of hydrocarbon source rock. Science in China (Earth Sciences) 51 (9), 1330–1339.
Florindo, F., Sagnotti, L., 1995. Palaeomagnetism and rock magnetism in the upper Pliocene Valle Ricca (Rome, Italy) section. Geophysical Journal International 123 (2), 340–354.
Garming, J.F.L., Bleil, U., Riedinger, N., 2005. Alteration of magnetic mineralogy at the sulphate–methane transition: analysis of sediments from the Argentine continental slope. Physics of the Earth and Planetary Interiors 151, 290–308.
Hendry, J.P., Pearson, M.J., Trewin, N.H., 2006. Jurassic septarian concretions from NW Scotland record interdependent bacterial, physical and chemical processes of marine mudrock diagenesis. Sedimentology 53, 537–565.
Hoffmann, V., 1992. Greigite (Fe_3S_4), magnetic properties and first domain observation. Physics of the Earth and Planetary Interiors 70, 288–301.
Horng, C.S., Chen, J.C., Lee, T.Q., 1992. Variations in magnetic minerals from two Plio-Pleistocene marine-deposited sections, southwestern Taiwan. Journal of Geological Society of China 35, 323–335.
Horng, C.S., Torri, M., Shea, K.S., Kao, S.J., 1998. Inconsistent magnetic polarities between greigite- and Pyrrhotite/magnetite-bearing marine sediments from the Tsailiaochi section, southwestern Taiwan. Earth and Planetary Science Letter 164, 467–481.
Housen, B.A., Musgrave, R.J., 1996. Rock-magnetic signature of gas hydrate in accretionary prism sediments. Earth and Planetary Science Letter 139, 509–519.
Hunger, S., Benning, L.G., 2007. Greigite: a true intermediate on the polysulfide pathway to pyrite. Geochemical Transaction 8 (1), http://dx.doi.org/10.1186/1467-4866-8-1.
Jiang, W.T., Horng, C.S., Roberts, A.P., Peacor, D.R., 2001. Contradictory magnetic polarities in sediments and variable timing of neoformation of authigenic greigite. Earth and Planetary Science Letter 193, 1–12.
Jiang, G.Q., Sohl, L.E., Christie-Blick, N., 2003a. Neoproterozoic stratigraphic comparison of the Lesser Himalaya (India) and Yangtze block (south China): paleogeographic implications. Geology 31, 917–920.
Jiang, G.Q., Kennedy, M.J., Christie-Blick, N., 2003b. Stable isotopic evidence for methane seeps in Neoproterozoic postglacial cap carbonates. Nature 426, 822–826.
Jiang, G.Q., Kennedy, M.J., Christie-Blick, N., Wu, H.C., Zhang, S.H., 2006a. Stratigraphy, sedimentary structures, and textures of the late Neoproterozoic Doushantuo cap carbonate in South China. Journal of Sedimentary Research 76, 978–995.
Jiang, G.Q., Shi, X.Y., Zhang, S.H., 2006b. Methane seeps, methane hydrate destabilization, and the late Neoproterozoic postglacial cap carbonates. Chinese Science Bulletin 51, 1152–1173.
Jiang, G.Q., Kaufman, A.J., Christie-Blick, N., Zhang, S.H., Wu, H.C., 2007. Carbon isotope variability across the Ediacaran Yangtze platform in South China: implications for a large surface-to-deep ocean δ13C gradient. Earth and Planetary Science Letters 261, 303–320.
Jiang, G.Q., Shi, X.Y., Zhang, S.H., Wang, Y., Xiao, S.H., 2011. Stratigraphy and paleogeography of the Ediacaran Doushantuo Formation (ca. 635–551 Ma) in South China. Gondwana Research 19, 831–849.
Kao, S.J., Horng, C.S., Roberts, A.P., Liu, K.K., 2004. Carbon–sulfur–iron relationships in sedimentary rocks from southwestern Taiwan: influence of geochemical environment on greigite and pyrrhotite formation. Chemical Geology 203, 153–168.
Karlin, R., 1990a. Magnetic mineral diagenesis in suboxic sediments at Bettis site W-N, NE Pacific Ocean. Journal of Geophysical Research 95, 4421–4436.
Karlin, R., 1990b. Magnetite diagenesis in marine sediments from the Oregon continental margin. Journal of Geophysical Research 95, 4405–4419.
Karlin, R., Levi, S., 1983. Diagenesis of magnetic minerals in recent haemipelagic sediments. Nature 303, 327–330.
Kasten, S., Freudenthal, T., Gingele, F.X., Schulz, H.D., 1998. Simultaneous formation of iron-rich layers at different redox boundaries in sediments of the Amazon deep-sea fan. Geochimica et Cosmochimica Acta 62 (13), 2253–2264.
Knoll, A.H., Walter, M.R., Narbonne, G.M., Christie-Blick, N., 2004. A new period for the geologic time scale. Science 305, 621–622.

Krupp, R.E., 1991. Smythite, greigite, and mackinawite: new observations on low-temperature iron sulfides. In: Pagel, M., Leroy, J.L. (Eds.), Source, Transport and Deposition of Metals. Balkema, Rotterdam, pp. 193–195.
Krupp, R.E., 1994. Phase relations and phase transformations between the low-temperature iron sulfides mackinawite, greigite, and smythite. European Journal of Mineralogy 6, 265–278.
Larrasoaña, J.C., Roberts, A.P., Musgrave, R.J., Gracia, E., Pinero, E., Vega, M., Martinéz-Ruiz, F., 2007. Diagenetic formation of greigite and pyrrhotite in gas hydrate marine sedimentary systems. Earth and Planetary Science Letter 261, 350–366.
Lash, G.G., Blood, D.R., 2004. Origin of shale fabric by mechanical compaction of flocculated clay: evidence from the upper Devonian Rhinestreet Shale, Western New York, USA. Journal of Sedimentary Research 74, 110–116.
Lee, C.H., Jin, J.H., 1995. Authigenic greigite in mud from the continental shelf of the Yellow sea, off the southwest Korean Peninsula. Marine Geology 128, 11–15.
Linder, J., Gilder, S.A., 2011. Geomagnetic secular variation recorded by sediments deposited during the Cretaceous normal superchron at low latitude. Physics of the Earth and Planetary Interiors 187, 245–260.
Liu, J., Zhu, R.X., Roberts, A.P., Li, S.Q., Chang, J.H., 2004. High-resolution analysis of early diagenetic effects on magnetic minerals in post-middle-Holocene continental shelf sediments from the Korea Strait. Journal of Geophysical Research 109, http://dx.doi.org/10.1029/2003JB002813.
Liu, P.J., Xiao, S.H., Yin, C.Y., Tang, F., Gao, L.Z., 2009. Silicified tubular microfossils from the upper Doushantuo Formation (Ediacaran) in the Yangtze Gorges Area, South China. Journal of Paleontology 83, 630–633.
McFadden, K.A., Huang, J., Chu, X., Jiang, G., Kaufman, A.J., Zhou, C., Yuan, X., Xiao, S., 2008. Pulsed oxidation and biological evolution in the Ediacaran Doushantuo Formation. Proceeding of the National Academy of Sciences 105 (9), 3197–3202.
McFadden, K.A., Xiao, S.H., Zhou, C.M., Kowalewski, M., 2009. Quantitative evaluation of the biostratigraphic distribution of acanthomorphic acritarchs in the Ediacaran Doushantuo Formation in the Yangtze Gorges area, South China. Precambrian Research 173, 170–190.
McKenzie, J.A., 1991. The dolomite problem: an outstanding controversy. In: Müller, D.W., McKenzie, J.A., Weissert, H. (Eds.), Controversies in modern geology, evolution of geological theories in sedimentology, earth history and tectonics. Academic Press, London, pp. 35–54.
Nash, M.C., Troitzsc, U., Opdyke, B.N., Trafford, J.M., Russell, B.D., Kline, D.I., 2011. First discovery of dolomite and magnesite in living coralline algae and its geobiological implications. Biogeosciences 8, 3331–3340.
Oda, H., Torri, M., 2004. Sea-level change and remagnetization of contimental shelf sediments off New Jersey (ODP Leg 174A): magnetite and greigite diagenesis. Geophysical Journal International 156, 443–458.
Pye, K., 1981. Marshrock formed by iron sulphide and siderite cementation in salt-marsh sediments. Nature 294, 650–652.
Raiswell, R., 1976. The microbiological formation of carbonate concretions in the upper Lias of N.E. England. Chemical Geology 18, 227–244.
Raiswell, R., 1982. Pyrite texture, isotopic composition and availability of iron. American Journal of Science 82, 1244–1263.
Raiswell, R., 1987. Non-steady state microbial diagenesis and the origin of carbonate concretions and nodular limestones. In: Marshall, J.D. (Ed.), Diagenesis of Sedimentary Sequences. Special Publication 36. Geological Society, London, pp. 41–54.
Raiswell, R., 1988. A chemical model for the origin of minor limestone-shale cycles by anaerobic methane oxidation. Geology 16, 641–644.
Raiswell, R., Fisher, Q.J., 2000. Mudrock-hosted carbonate concretions: a review of growth mechanisms and their influence on chemical and isotopic composition. Journal of the Geological Society, London 157, 239–251.
Reynolds, R.L., Tuttle, M.L., Rice, C.A., Fishman, N.S., Karachewski, J.A., Sherman, D.M., 1994. Magnetization and geochemistry of greigite-bearing Cretaceous strata, North Slope basin, Alaska. American Journal of Science 294, 485–528.
Reynolds, R.L., Rosenbaum, J.G., van Metre, P., Tuttle, M., Callender, E., Goldin, A., 1999. Greigite as an indicator of drought – the 1912–1994 sediment magnetic record from White Rock Lake, Dallas, Texas, USA. Journal of Paleolimnology 21, 193–206.
Roberts, A.P., 1995. Magnetic properties of sedimentary greigite (Fe_3S_4). Earth and Planetary Science Letter 134, 227–236.
Roberts, A.P., Turner, G.M., 1993. Diagenetic formation of ferromagnetic iron sulphide minerals in rapidly deposited marine sediments, South Island, New Zealand. Earth and Planetary Science Letter 115 (1), 257–273.
Roberts, A.P., Weaver, R., 2005. Multiple mechanisms of remagnetization involving sedimentary greigite (Fe_3S_4). Earth and Planetary Science Letter 231, 263–277.
Roberts, J.A., Bennett, P.C., González, L.A., Macpherson, G.L., Milliken, K.L., 2004. Microbial precipitation of dolomite in methanogenic groundwater. Geology 32, 277–280.
Roberts, A.P., Jiang, W.T., Florindo, F., Horng, C.S., Laj, C., 2005. Assessing the timing of greigite formation and the reliability of the upper Olduvai polarity transition record from the Crostolo River, Italy. Geophysical Research Letters 32, L05307, http://dx.doi.org/10.1029/2004GL022137.
Rowan, C.J., Roberts, A.P., 2005. Tectonic and geochronological implications of variably timed magnetizations carried by authigenic greigite in marine sediments from New Zealand. Geology 33, 553–556.
Rowan, C.J., Roberts, A.P., 2006. Magnetite dissolution, diachronous greigite formation, and secondary magnetizations from pyrite oxidation: Unravelling complex magnetizations in Neogene marine sediments from New Zealand. Earth and Planetary Science Letter 241, 119–137.
Rowan, C.J., Roberts, A.P., 2008. Widespread remagnetizations and a new view of tectonic rotations within the Australia-Pacific plate boundary zone, New Zealand. Journal of Geophysical Research 113, B03103, http://dx.doi.org/10.1029/20065B004594.
Rowan, C.J., Roberts, A.P., Broadbent, T., 2009. Reductive diagenesis, magnetite dissolution, greigite growth and paleomagnetic smoothing in marine sediments: a new view. Earth and Planetary Science Letter 277, 223–235.
Russell, M.J., Hall, A.J., 1997. The emergence of life from iron monosulphide bubbles at a submarine hydrothermal redox and pH front. Journal of the Geological Society, London 154, 377–402.
Russell, M.J., Daniel, R.M., Hall, A.J., Sherringham, J., 1994. A hydrothermally precipitated catalytic iron sulphide membrane as a first step toward life. Journal of Molecular Evolution 39, 231–243.
Sagnotti, L., Winkler, A., 1999. Rock magnetism and palaeomagnetism of greigite-bearing mudstones in the Italian peninsula. Earth and Planetary Science Letter 165, 67–80.
Sagnotti, L., Winkler, A., Weaver, R., Verosub, K.L., Florindo, F., Pike, C.R., Clayton, T., Wilson, G.S., 2005. Apparent magnetic polarity reversals due to remagnetization resulting from late diagenetic growth of greigite from siderite. Geophysical Journal International 160, 89–100.
Skinner, B.J., Erd, R.C., Grimaldi, F.S., 1964. Greigite, the thio-spinel of iron: a new mineral. American Mineralogist 49, 543–555.
Snowball, L., 1991. Magnetic hysteresis properties of greigite (Fe_3S_4) and a new occurrence in Holocene sediments from Swedish Lappland. Physics of the Earth and Planetary Interiors 68, 32–40.
Snowball, I., Thompson, R., 1988. The occurrence of greigite in sediments from Loch Lomond. Journal of Quaternary Science 3 (2), 121–125.
Tarduno, J.A., 1995. Superparamagnetism and reduction diagenesis in pelagic sediments-enhancement or depletion? Geophysical Research Letters 22, 1337–1340.
Vasconcelos, C., McKenzie, J.A., 1997. Microbial mediation of modern dolomite precipitation and diagenesis under anoxic conditions (Lagoa Vermelha, Rio de Janeiro, Brazil). Journal of Sedimentary Research 67, 378–390.
Vasconcelos, C., McKenzie, J.A., Bernasconi, S., Grujic, D., Tien, A.J., 1995. Microbial mediation as a possible mechanism for natural dolomite formation at low temperatures. Nature 377, 220–222.
Wang, J., Li, Z.X., 2003. History of Neoproterozoic rift basins in South China: implications for Rodinia break-up. Precambrian Research 122 (1–4), 141–158.
Weaver, R., Roberts, A.P., Barker, A.J., 2002. A late diagenetic (synfolding) magnetization carried by pyrrhotite: implications for paleomagnetic studies from magnetic iron sulphide-bearing sediments. Earth and Planetary Science Letter 200, 371–386.
Wilkin, R.T., Barnes, H.L., 1997. Formation processes of framboidal pyrite. Geochimica et Cosmochimica Acta 61, 323–339.
Woodland, B.G., 1984. Microstructure of agglomerated suspended sediments in Northern Chesapeake Bay Estuary. Science 202, 49–51.
Xiao, S., 2004. New multicellular algal fossils and acritarchs in Doushantuo chert nodules (Neoproterozoic; Yangtze Gorges area, South China). Journal of Paleontology 78, 393–401.
Xiao, S.H., Yuan, X.L., Steiner, M., Knoll, A.H., 2002. Macroscopic carbonaceous compressions in a terminal Proterozoic shale: a systematic reassessment of the Miaohe biota, South China. Journal of Paleontology 76, 347–376.
Yamazaki, T., Abdeldayem, A.L., Ikehara, K., 2003. Rock-magnetic changes with reduction diagenesis in Japan Sea sediments and preservation of geomagnetic secular variation in inclination during the last 30,000 years. Earth Planets Space 55, 327–340.
Yin, L.M., Zhu, M.Y., Knoll, A.H., Yuan, X.L., Zhang, J.M., Hu, J., 2007. Doushantuo embryos preserved inside diapause egg cysts. Nature 446, 661–663.
Zabawa, C.F., 1978. Microstructure of agglomerated suspended sediments in Northern Chesapeake Bay Estuary. Science 202, 49–51.
Zhang, Y., Yin, L., Xiao, S., Knoll, A.H., 1998. Permineralized fossils from the terminal Proterozoic Doushantuo Formation, South China. The Plaeontological Society Memoir 50, 1–52.
Zhang, S.H., Jiang, G.Q., Zhang, J.M., Song, B., Kennedy, M.J., Christie-Blick, N., 2005. U–Pb sensitive high-resolution ion microprobe ages from the Doushantuo Formation in South China: constraints on late Neoproterozoic glaciations. Geology 33, 473–476.
Zhang, Q.R., Li, X.H., Feng, L.J., Huang, J., Song, B., 2008a. A new age constraint on the onset of the Neoproterozoic glaciations in the Yangtze Platform, South China. The Journal of Geology 116, 423–429.
Zhang, S.H., Jiang, G.Q., Dong, J., Han, Y.G., Wu, H.C., 2008b. The New SHRIMP age of the Wuqiangxi Formation of Banxi Group: implications for rifting and stratigraphic erosion associated with the early Cryogenian (Sturtian) glaciation in South China. Science in China (Earth Sciences) 51 (11), 1537–1544.
Zhang, S.H., Jiang, G.Q., Han, Y.G., 2008c. The age of the Nantuo formation and Nantuo glaciation in South China. Terra Nova 20 (4), 289–294.
Zhou, C.M., Xie, G.W., McFadden, K., Xiao, S.H., Yuan, X.L., 2007. The diversification and extinction of Doushantuo-Pertatataka acritarchs in South China: causes and biostratigraphic significance. Geological Journal 42, 229–262.
Zhu, M., Zhang, J., Steiner, M., Yang, A., Li, G., Erdtmann, B.D., 2003. Sinian and early Cambrian stratigraphic frameworks from shallow- to deep-water facies of the Yangtze Plaform: an integrated approach. Progress in Natural Science 13 (12), 951–960.
Zhu, M., Strauss, H., Shields, G.A., 2007. From snowball earth to the Cambrian bioradiation: calibration of Ediacaran-Cambrian earth history in South China. Palaeogeography, Palaeoclimatology, Palaeoecology 254 (1–2), 1–6.